Applied Catalysis B: Environmental 98 (2010) 213–223

Contents lists available at ScienceDirect

Applied Catalysis B: Environmental

journal homepage: www.elsevier.com/locate/apcatb

Hydrodeoxygenation of 2-ethylphenol as a model compound of bio-crude over sulfided Mo-based catalysts: Promoting effect and reaction mechanism

Y. Romero, F. Richard*, S. Brunet

Laboratoire de catalyse en chimie organique, UMR 6503, Faculté des Sciences Fondamentales et Appliquées, Université de Poitiers, 40, avenue du Recteur Pineau, F-86022 Poitiers Cedex, France

ARTICLE INFO

Article history:
Received 3 March 2010
Received in revised form 26 May 2010
Accepted 28 May 2010
Available online 8 June 2010

Keywords:
Hydrodeoxygenation
NiMo
CoMo
2-Ethylphenol
Promoting effect

ABSTRACT

The hydrodeoxygenation of 2-ethylphenol was carried out under 7 MPa of total pressure and at 340 °C in a fixed-bed reactor over unpromoted Mo/Al_2O_3 catalyst and over two promoted catalysts ($CoMo/Al_2O_3$ and $NiMo/Al_2O_3$). For all experiments, dimethyldisulfide was added to the feed to maintain the sulfidation state of the catalysts. On these sulfided catalysts, the transformation of 2-ethylphenol is considered to proceed by three pathways: (1) prehydrogenation of the aromatic ring followed by a dehydration reaction leading to a mixture of alkenes (1-ethylcyclohexene and 3-ethylcyclohexene) and after hydrogenation leading to ethylcyclohexane (HYD pathway); (2) direct cleavage of the C_{sp2}–O bond leading to ethylbenzene (DDO pathway); (3) disproportionation and isomerization reactions leading to oxygenated products (phenol, isomers of 2-ethylphenol and diethylphenols) and their deoxygenated products (ACI pathway). The production of those oxygenated compounds mainly involved the support acidity. The presence of nickel and cobalt allowed an increase of the deoxygenation rate. Nickel only promoted the HYD pathway whereas cobalt promoted both the HYD and DDO pathways. Consequently, the DDO/HYD selectivity was very dependent on the catalyst used. The highest DDO/HYD selectivity was obtained for $CoMo/Al_2O_3$. Sulfur vacancies are proposed as active sites for both deoxygenation pathways of 2-ethylphenol, although other active sites (e.g. brim sites) could be involved to explain that the HYD pathway was always predominant. For both deoxygenation pathways, two probable mechanisms are described. The adsorption mode of the molecule most likely determines the deoxygenation route.

1. Introduction

The worldwide energy demand continues to rise because of two main reasons: (1) the ongoing increase in world population, and (2) the growing demand by the developing countries to improve their standards of living. In addition, the fossil fuels, which meet most of the world's energy demand today, are being depleted fast [1]. Under this scenario the development of new liquid fuels coming from biomass is an attractive alternative [2]. The European Union is committed to use non-food cellulosic and ligno-cellulosic biomass as a sustainable alternative for bio-fuel production [3]. This kind of feedstock, unlike those from fossil fuels, has a high oxygen content (between 20 and 55 wt%) depending on the biomass source and the transformation process used [4–10]. A lot of oxygenated functions are observed in these oils such as acid, aldehyde, alcohol and phenolic groups [10–12]. For example, Marsman et al. [12] gave the composition of a beech pyrolysis oil which contained about 20 wt% of acids, 35 wt% of aromatic compounds (such as guaiacols and phenolic compounds), 15 wt% of alcohols and 20 wt% of sugars. These oxygenated compounds are responsible for some detrimental properties of bio-oil such as high viscosity, low volatility, corrosiveness, immiscibility with fossil fuels, thermal instability and tendency to polymerize under exposure to air. Therefore, bio-oil upgrading to liquid fuel requires oxygen removal by a catalytic hydrodeoxygenation (HDO) in which oxygen is taken out in the form of water and/or carbon oxides under a high pressure of hydrogen [13]. To upgrade these bio-fuels without changing drastically the processing conditions, the use of sulfided Mo/Al_2O_3 catalysts, promoted by sulfides of group VIII (Co, Ni), is required. The presence of cobalt or nickel is known to increase the activity of molybdenum sulfide catalysts for hydrotreating reactions [14]. The model based on the so-called "Co(Ni)–Mo–S" structure proposed by Topsøe and coworkers [15–17] is most widely accepted nowadays to explain this promoting effect. It was proposed that the promoter (Ni or Co) donates electrons to molybdenum and leads to a weakening of the metal–sulfur bond [18,19]. The active site in these catalysts is accepted to be a sulfur vacancy (coordinatively unsaturated site: CUS) present on the edges of the MoS_2 slabs.

In most of the studies on hydrodeoxygenation reactions, phenolic compounds were used as model molecules [20–32]. Over

* Corresponding author. Tel.: +33 05 49 45 35 19; fax: +33 05 49 45 38 99.
E-mail address: frederic.richard@univ-poitiers.fr (F. Richard).

0926-3373/$ – see front matter © 2010 Elsevier B.V. All rights reserved.
doi:10.1016/j.apcatb.2010.05.031

sulfided catalysts, it is generally accepted that phenolic compounds react through two pathways: one involving direct C–O bond scission (direct deoxygenation route – DDO) yielding aromatic products, and the other via prehydrogenation of the aromatic ring leading to cycloalkenes and cycloalkanes (HYD pathway) [20,22–25,27–29,32]. The latter pathway involves an alcohol as intermediate. When 2-ethylphenol (2-EtPh) was used as reactant, a third pathway was observed over a NiMoP/Al_2O_3 catalyst, leading to oxygenated products which involved the acid properties of the catalyst [32]. These oxygenated products were obtained by disproportionation and isomerization reactions. In the presence of cobalt as promoter, the DDO pathway was the main route of hydrodeoxygenation of phenolic compounds [20,22,24,27], whereas in the presence of nickel as promoter, the HYD pathway was always the more prominent [23,24,29,31,32]. For example, Laurent and Delmon [24] studied the transformation of 4-methylphenol in a batch reactor at 340 °C under 7 MPa of total pressure over sulfided NiMo and CoMo catalysts. In the presence of CS_2 as sulfiding agent in the feed to maintain the sulfided form of the catalyst, the authors reported that NiMo/Al_2O_3 was about twice as active as CoMo/Al_2O_3 in hydrodeoxygenation. In addition, the HYD/DDO ratio was 0.9 when cobalt was used as promoter and 20 in the presence of nickel. Under 1.5 MPa of total pressure at 250 °C in a flow reactor, Senol et al. [29] observed that CoMo/Al_2O_3 was more active than NiMo/Al_2O_3 for the hydrodeoxygenation of phenol. Benzene, obtained by the DDO pathway, was the major product over CoMo, whereas cyclohexane (the main HYD product) was the major product over NiMo. It was also reported that the DDO pathway is predominantly affected by steric hindrance of alkyl groups adjacent to the OH group [20,22,25]. Furthermore, 2-ethylphenol was the main oxygenated product observed during the transformation of benzofuran over sulfided catalysts [32–38]. It was also observed an inhibiting effect of benzofuranic compounds on the hydrodeoxygenation of 2-ethylphenol due to a competitive adsorption between these two types of compounds on the deoxygenation active sites [32,34].

As indicated above, nearly all the results reported on the hydrodeoxygenation of model oxygenated molecules over sulfided catalysts were obtained with NiMo/Al_2O_3 and/or CoMo/Al_2O_3. While the importance of the promoting effect is well quantified for hydrodesulfurization and hydrodenitrogenation [14], it appears that such data are not available for hydrodeoxygenation reactions. The aim of this paper is to evaluate the promoting effect of nickel and cobalt and to determine their influence on the two main hydrodeoxygenation pathways of phenolic compounds.

In this paper we examined the effect of cobalt and nickel promoters on the activity of a Mo/Al_2O_3-based catalyst in the hydrodeoxygenation of 2-ethylphenol used as an oxygenated model molecule. Its transformation was carried out in a fixed-bed reactor under conditions close to hydrotreatment process conditions (7 MPa and 340 °C) in the presence of H_2S to maintain the sulfidation level of the catalyst during the hydrodeoxygenation process. In order to evaluate the influence of the support, the activity and selectivity of γ-Al_2O_3 was studied under the same experimental conditions. Our aim is to discuss the nature of the catalytic active sites and the mechanisms involved during the hydrodeoxygenation over typical hydrotreating catalysts, and more particularly to identify if the DDO and HYD pathways occur on the same or on distinct catalytic centers.

Table 2
Average stacking and particle size of sulfided catalysts measured by TEM analysis.

Catalyst	Size (nm)	Stacking
MoS_2/γ-Al_2O_3	3.3	2.0
CoMoS/γ-Al_2O_3	3.1	1.6
NiMoS/γ-Al_2O_3	2.2	1.2

2. Experimental

2.1. Chemical materials

2-Ethylphenol (2-EtPh, 99%), dimethyldisulfide (DMDS, 98%) and toluene (99%) were purchased from Aldrich and used without further purification.

2.2. Catalysts

All the catalysts (γ-Al_2O_3, Mo/γ-Al_2O_3, NiMo/γ-Al_2O_3, CoMo/γ-Al_2O_3) were supplied by TOTAL. Textural properties of catalysts and supports were determined by nitrogen physisorption on an ASAP 2000 Micromeritics instrument. The specific surface area was calculated from the linear portion of BET plots (P/P_0 = 0.05–0.30) and the pore volume at P/P_0 = 0.99. The cobalt and nickel composition was measured by XRF and the molybdenum content by ICP. The catalyst composition and the textural properties of the support (γ-Al_2O_3) and catalysts in the oxidic form are given in Table 1. For all catalysts, the same alumina was used. All catalysts have comparable textural properties and/or Mo and promoter content.

The acidity of the support was measured in absence of H_2S by IR spectroscopy of adsorbed pyridine (Nicolet Magna IR 550 Fourier transform spectrometer). The concentration of the Lewis acid sites (258 μmol g^{-1}) able to retain pyridine at 150 °C was determined by using the band at 1450 cm^{-1} with the extinction coefficient of 1.28 cm μmol^{-1}. No Brønsted acid sites were observed.

TEM analysis was performed on a Philips CM 120 instrument operating at 120 kV. Samples were dispersed in ethanol and deposited on a Cu grid previously covered with a thin layer of carbon. At least 25 micrographs (each corresponding to about 2700 nm^2) were evaluated, corresponding to about 200 particles, for each sulfided catalyst (Mo/Al_2O_3, CoMo/Al_2O_3 and NiMo/Al_2O_3). Particle sizes were similar for sulfided Mo/Al_2O_3 and CoMo/Al_2O_3 (near 3.2 nm) and were lower for sulfided NiMo/Al_2O_3 (Table 2). The stacking was also lower for NiMo compared to the two other catalysts. The presence of Ni_3S_2 or Co_9S_8 crystallites was not observed.

The percentages of carbon and sulfur present on the catalysts after the sulfidation step and after reaction were obtained by using an elementary analyzer (NA2100 analyzer, CE instruments). Before these analyses, the weakly adsorbed organic compounds over spent catalysts were eliminated by a Soxhlet extraction with dichloromethane.

Table 1
Chemical composition, BET area and pore volume of the catalysts.

	γ-Al_2O_3	Mo/γ-Al_2O_3	CoMo/γ-Al_2O_3	NiMo/γ-Al_2O_3
BET area (m^2/g)	252	251	255	257
Pore volume (cm^3/g)	0.85	0.70	0.64	0.66
Mo (wt%)	–	9.9	9.2	9.3
Co (wt%)	–	–	4.2	–
Ni (wt%)	–	–	–	3.9

Table 3
Partial pressures of the various compounds in sulfidation and reaction conditions.

	P_{total} (MPa)	P_{H_2} (MPa)	$P_{toluene}$ (MPa)	$P_{2\text{-EtPh}}$ (kPa)	P_{H_2S} (kPa)	P_{CH_4} (kPa)
Sulfidation conditions	4	2.674	1.068	–	129	129
Reaction conditions	7	5.750	1.103	49	49	49

2.3. Sulfidation and reaction conditions

All the samples (support and catalysts) were sulfided in situ into a dynamic flow reactor using a mixture of 5.8 wt% dimethyldisulfide (DMDS) in toluene, under a 4.0 MPa total pressure (Table 3). The sulfiding mixture was injected at a starting temperature of 150 °C. After 1 h, the temperature was raised to 350 °C at a rate of 5 °C/min and it was maintained at 350 °C for 14 h. The temperature was then lowered to the reaction temperature (340 °C). The particle size of the catalysts was in the range of 250–315 μm. The catalysts were diluted in carborundum to keep the volume of the catalytic bed constant.

The catalytic test was carried out in a high-pressure fixed-bed microreactor (length: 40 cm; inner diameter: 1.25 cm) at 340 °C, under 7 MPa of total pressure after in situ sulfidation of the catalyst according to the procedure described above. The oxygenated model compound (2-EtPh) was diluted in toluene and DMDS (2.1 wt% S) was added to generate H_2S in situ during the reaction. The partial pressure of 2-EtPh was maintained at 49 kPa and the pressure of hydrogen was 5.75 MPa (Table 3). The contact time, defined as the ratio between the volume of catalyst and the gas flow of 2-EtPh, was varied by changing the flow rates of the liquid and the gaseous reactants. This contact time was varied between 1.7 and 9.3 min (liquid feed flow = 5.1–28 mL h^{-1} and H_2 flow = 5.7–32.1 L h^{-1}) when Al_2O_3 was tested as catalyst. It was between 1.5 and 9.3 min (liquid feed flow = 4.5–28.0 mL h^{-1} and H_2 flow = 5.1–31.8 L h^{-1}) for MoS_2/Al_2O_3 and between 0.6 and 6.1 min (liquid feed flow = 3.0–30.0 mL h^{-1} and H_2 flow = 3.4–34.0 L h^{-1}) for both promoted catalysts. In order to obtain comparable conversions, 50 mg of promoted catalyst or 100 mg of unpromoted catalyst were used.

Methylcyclohexane obtained from toluene hydrogenation was observed in very low quantities: less than 1 mol% whatever the contact time used.

2.4. Chromatographic analysis

The reactor effluents were condensed and liquid samples were periodically collected and analyzed with a Varian 3300 chromatograph equipped with a DB1 capillary column (length: 30 m; inside diameter: 0.50 mm; film thickness: 0.25 μm) and a flame ionization detector. The oven temperature was programmed from 55 °C (maintained for 5 min) to 175 °C (4 °C/min). The products were identified by using GC/MS analysis (Finnigan INCOS 500) and by co-injection of commercial samples provided by Aldrich. Gaseous products were not found except for methane which was produced by DMDS decomposition. For the quantification analysis, response factors for the reactant and the products were determined and tested against model solutions of known concentrations.

The total catalyst activity (global reaction rate) was calculated according to the following equation:

$$A_{tot} = \frac{XF}{W}$$

where A_{tot} is the total activity of the catalyst (mmol g^{-1} h^{-1}), X the conversion of the reactant, F the molar flow rate of 2-EtPh (mmol h^{-1}) and W the weight of catalyst (g). That equation has been used only for conversion lower than 20 mol%. All conversions were measured after catalyst stabilization.

3. Results

3.1. Transformation of 2-ethylphenol over γ-Al_2O_3

Over γ-Al_2O_3, 2-EtPh was transformed through disproportionation and isomerization reactions involving the acid properties of the support. An important deactivation of the catalyst was observed with time on stream. Indeed, for a contact time of 2.3 min, the initial conversion of 2-EtPh was 37 mol% but it dropped to 20 mol% after 30 h on stream.

The product distribution at various conversion rates was obtained by changing the contact time. The disproportionation products appeared as primary products whereas the isomerization products were observed as secondary products (Fig. 1). Disproportionation led to phenol and diethylphenols in equal amounts. All of the possible six diethylphenol isomers were observed: 2,4-diethylphenol, 2,5-diethylphenol and 2,6-diethylphenol appeared as primary products (Fig. 2). The other diethylphenol isomers

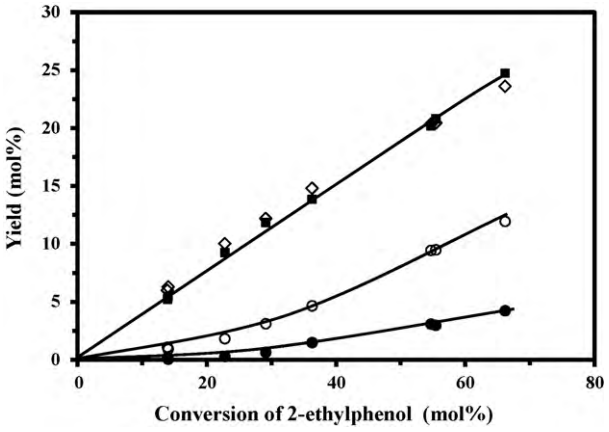

Fig. 1. Transformation of 2-ethylphenol over γ-Al_2O_3 at 340 °C under 7 MPa of total pressure. Effect of the conversion of 2-ethylphenol on the product distribution. Phenol (■); diethylphenol isomers (◊); 3-ethylphenol (○); 4-ethylphenol (●).

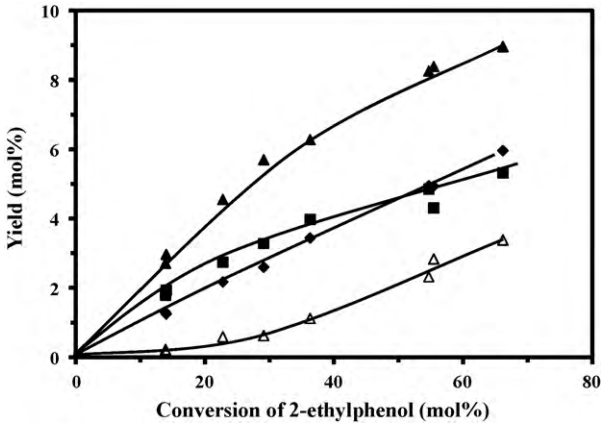

Fig. 2. Transformation of 2-ethylphenol over γ-Al_2O_3 at 340 °C under 7 MPa of total pressure. Effect of the conversion of 2-ethylphenol on the formation of diethylphenols. 2,5-Diethylphenol (▲); 2,6-diethylphenol (■); 2,4-diethylphenol (♦); other diethylphenol isomers (△).

Table 4
Chemical composition in carbon and sulfur of sulfided and spent catalysts. Spent catalysts were obtained after 30 h on stream for 2-EtPh transformation at 340 °C under 7 MPa of total pressure.

	%C	%S
Sulfided catalysts		
$Mo/\gamma\text{-}Al_2O_3$	1.3	5.3
$CoMo/\gamma\text{-}Al_2O_3$	1.2	7.4
$NiMo/\gamma\text{-}Al_2O_3$	0.4	7.9
Spent catalysts		
$Mo/\gamma\text{-}Al_2O_3$	3.9	5.1
$CoMo/\gamma\text{-}Al_2O_3$	3.3	7.2
$NiMo/\gamma\text{-}Al_2O_3$	3.0	6.6

(2,3-diethylphenol, 3,4-diethylphenol and 3,5-diethylphenol) were secondary products. In addition, both isomers of 2-EtPh (3-ethylphenol and 4-ethylphenol) were observed and appeared as secondary products (Fig. 1). Whatever the conversion of 2-EtPh, 3-ethylphenol was always observed in greater quantities than 4-ethylphenol. Indeed, for 66 mol% of 2-EtPh conversion, the yield in 3-ethylphenol and 4-ethylphenol was 12 mol% and 4 mol%, respectively. It was also observed that the disproportionation/isomerization (*D*/*I*) ratio decreased with the conversion of 2-EtPh. This ratio was equal to 12 for 14 mol% of 2-EtPh conversion and decreased to 2.4 for 70 mol% of 2-EtPh conversion. In addition to these products, methanethiol, dimethylsulfide and methane which resulted from the decomposition of DMDS were also detected.

3.2. Transformation of 2-ethylphenol over Mo/Al_2O_3

Over Mo/Al_2O_3, in addition to the oxygenated products formed on alumina as reported above, deoxygenated products were observed. This sulfided catalyst was more stable than alumina. Indeed, for a contact time of 2.3 min, the initial conversion of 2-EtPh was 27 mol% and was 22 mol% after 30 h on stream. The carbon and sulfur contents of this catalyst were reported in Table 4. The total amount of sulfur over the unpromoted catalyst after sulfidation and after reaction was similar and close to 5.2 wt% showing that the addition of H_2S in the feed allowed to maintain the sulfidation state of this catalyst. Regarding the carbon content, it was close to 4 wt% after 30 h on stream, indicating that the coke formation over the unpromoted catalyst could be responsible of the slight catalyst deactivation observed.

Three main transformation pathways of 2-EtPh on the unpromoted sulfided catalyst were identified (Fig. 3). The first one corresponds to the products formed by the hydrogenation pathway

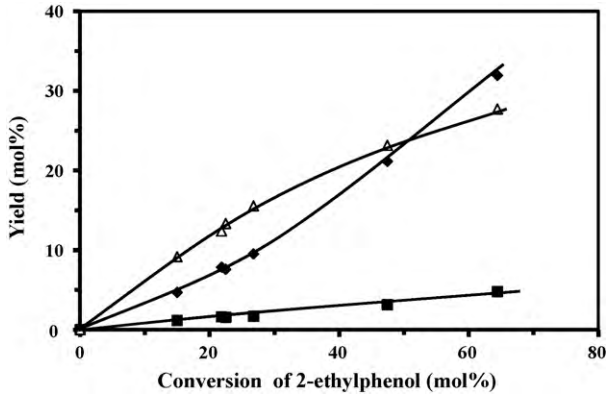

Fig. 3. Transformation of 2-ethylphenol over sulfided $Mo/\gamma\text{-}Al_2O_3$ catalyst at 340 °C under 7 MPa of total pressure. Effect of the conversion of 2-ethylphenol on the product distribution. ACI pathway (△); HYD pathway (♦); DDO pathway (■).

Table 5
Activity for the transformation of 2-EtPh over alumina and sulfided Mo-based catalysts at 340 °C under 7 MPa of total pressure. Promoting effect of Ni and Co (in brackets, defined as the activity of promoted catalysts over unpromoted catalyst ratio).

	$\gamma\text{-}Al_2O_3$	$Mo/\gamma\text{-}Al_2O_3$	$CoMo/\gamma\text{-}Al_2O_3$	$NiMo/\gamma\text{-}Al_2O_3$
Activity (mmol g^{-1} h^{-1})				
Total[a]	15.0	17.0	28.0 (1.6)	30.8 (1.8)
HDO[b]	0	8.3	19.0 (2.3)	23.1 (2.8)
HYD[c]	0	5.7	11.4 (2.0)	19.3 (3.4)
DDO[d]	0	1.2	4.6 (3.8)	1.4 (1.2)
ACI[e]	15.0	10.1	12.0 (1.2)	10.1 (1.0)

[a] Activity taking into account the global rate of 2-EtPh transformation.
[b] Activity in total deoxygenation.
[c] Hydrogenation pathway (HYD).
[d] Direct deoxygenation pathway (DDO).
[e] Acidic pathway (ACI).

(HYD products: ethylcyclohexane, 1-ethylcyclohexene and 3-ethylcyclohexene), the second corresponds to the product formed by the direct deoxygenation pathway (DDO product: ethylbenzene) and the third one involves the acidic and the deoxygenating properties of the catalyst (ACI products: phenol, diethylphenols, 3-ethylphenol and their deoxygenated products).

Table 5 shows that the total activity of alumina was about the same as that of Mo/Al_2O_3, but the activity according to the ACI pathway of the latter was lower than that of alumina. This could probably be due to a decrease in the number of acid sites accessible because of the presence of the sulfide phase.

For a 2-EtPh conversion lower than 30 mol%, Fig. 3 shows a linear behavior for the yield of HYD, DDO and ACI products vs the conversion of 2-EtPh, indicating that those primary products were formed through parallel reactions. At a higher conversion, the loss of linearity for the two main routes (HYD and ACI pathways) was due to the deoxygenation of ACI products into HYD products. Indeed, 3-ethylphenol which was formed by the ACI pathway on alumina, as indicated earlier, led to the same deoxygenated products than 2-EtPh, which was mainly ethylcyclohexane. Over unpromoted catalyst, the DDO pathway was always in minor importance compared to HYD and ACI pathways. Ethylbenzene was the only product obtained through the DDO pathway. Its yield increased linearly with 2-EtPh conversion, indicating that ethylbenzene was not hydrogenated into ethylcyclohexane under our experimental conditions. Indeed, we verified that ethylbenzene was unreactive at 340 °C under 7 MPa of total pressure.

Table 6 shows the product distribution obtained for the 2-EtPh conversion close to 20 mol% for all the sulfided catalysts studied. Over the unpromoted catalyst, the deoxygenated products constituted about half of the total products. The products formed by the HYD pathway were 1-ethylcyclohexene, 3-ethylcyclohexene and ethylcyclohexane which was always the main product of this pathway for a 2-EtPh conversion over 20 mol% (Fig. 4). The alkenes (1-ethylcyclohexene and 3-ethylcyclohexene) were obtained as primary products and afterwards hydrogenated into ethylcyclohexane. The alkenes were probably formed from 2-ethylcyclohexanol which is the totally hydrogenated product of 2-EtPh. However, this alcohol was never observed under our experimental conditions.

The transformation of 2-ethylcyclohexanol was carried out on alumina using the same reaction conditions. We observed that 2-ethylcyclohexanol was totally converted into 1-ethylcyclohexene (1-EtCyHe) and 3-ethylcyclohexene (3-EtCyHe). The 1-EtCyHe/3-EtCyHe ratio obtained here was close to the one observed during the transformation of 2-EtPh on sulfided $Mo/\gamma\text{-}Al_2O_3$ (3 vs 2.8).

As indicated above, the only product obtained through the DDO pathway was ethylbenzene. For 22 mol% of 2-EtPh conversion, it represented only 7 mol% of all products observed over this catalyst

Table 6
Transformation of 2-ethylphenol over sulfided Mo-based catalyst at 340 °C under 7 MPa of total pressure. Effect of the catalyst on the conversion and on the product distribution.

	$Mo/\gamma\text{-}Al_2O_3$	$CoMo/\gamma\text{-}Al_2O_3$	$NiMo/\gamma\text{-}Al_2O_3$
Contact time (min)	2.30	1.15	1.11
2-EtPh conversion (mol%)	22.0	24.0	23.0
HDO yield[a] (mol%)	11.3	17.0	18.8
DDO/HYD selectivity	0.2	0.4	0.1
Product distribution (mol%)			
HYD pathway			
Ethylcyclohexane	20.4	29.2	47.6
1-Ethylcyclohexene	11.5	9.9	15.4
3-Ethylcyclohexene	4.1	3.6	5.3
DDO pathway			
Ethylbenzene	7.4	17.7	4.4
ACI pathway			
Oxygenated compounds			
Phenol	20.1	11.0	7.2
3-Ethylphenol	6.2	2.3	1.4
2,6-Diethylphenol	11.1	7.6	5.4
2,4-Diethylphenol	2.9	1.7	1.2
2,5-Diethylphenol	7.6	4.8	3.4
Other diethylphenol isomers	0.5	0.3	0.5
Deoxygenated compounds			
1,3-Diethylbenzene	0.5	1.1	0.2
1,4-Diethylbenzene	0.6	1.7	0.1
Diethylcyclohexane isomers	1.0	1.1	1.5
Cyclohexane	2.2	3.5	3.5
Cyclohexene	3.2	3.2	2.3
Benzene	0.7	1.3	0.6

[a] HDO yield: yield in all deoxygenated products.

(Table 6). The DDO/HYD selectivity measured over the unpromoted catalyst was 0.2.

The ACI pathway was the most important route for the 2-EtPh conversion under 50 mol% over the Mo/Al_2O_3 catalyst (Fig. 3). This pathway includes both oxygenated products (phenol, diethylphenol isomers and 3-ethylphenol) and their deoxygenated products. The oxygenated products were formed exclusively by acid catalysis (isomerization and disproportionation products) involving mainly the acid sites of the support. However, in the presence of the sulfided phase, a fraction of these products were transformed into deoxygenated products by HYD and DDO pathways. Cyclohexene and cyclohexane were obtained from the HYD pathway of phenol, whereas benzene was obtained by its DDO pathway. The latter was observed in very low quantities compared to the HYD products of phenol (cyclohexene and cyclohexane). Indeed, the phenol DDO/HYD selectivity was about 0.1, lower than that obtained for the 2-EtPh transformation (equal to 0.2). The deoxygenation of the diethylphenol isomers led to several diethylcyclohexane isomers obtained by the HYD route. In addition, 1,3-diethylbenzene and 1,4-diethylbenzene were also detected and formed by the DDO route of diethylphenols, probably from 2,4-diethylphenol and 2,5-diethylphenol, respectively. Although, 2,5-diethylphenol was the major diethylphenol obtained through disproportionation on alumina (Fig. 2), 2,6-diethylphenol appeared as the main diethylphenol isomers over sulfided catalysts. This suggests a likely steric hindrance of ethyl groups on deoxygenation as already reported for the HDO of dimethyl phenols [22,25]. It seems that phenol was more reactive by deoxygenation than the diethylphenol isomers, since the deoxygenated products coming from phenol were always in larger amount than those coming from diethylphenols, as indicated in Table 6 and Fig. 5.

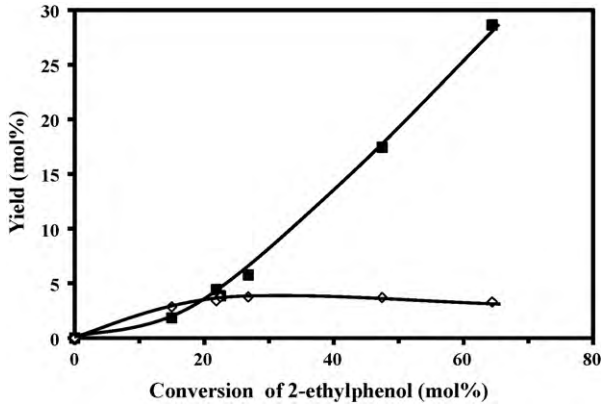

Fig. 4. Transformation of 2-ethylphenol over sulfided $Mo/\gamma\text{-}Al_2O_3$ catalyst at 340 °C under 7 MPa of total pressure. Effect of the conversion of 2-ethylphenol on the formation of HYD products. Ethylcyclohexane (■); ethylcyclohexenes (◊).

3.3. *Effect of Ni or Co promoters on the transformation of 2-ethylphenol*

The transformation of 2-EtPh was also studied on $CoMo/Al_2O_3$ and $NiMo/Al_2O_3$ and the results were compared to those obtained with the unpromoted catalyst (Mo/Al_2O_3) under the same experimental conditions (7 MPa and 340 °C). For a contact time of 2.2 min, the initial conversion of 2-EtPh over $CoMo/Al_2O_3$ was 39 mol% and was 36 mol% (8% loss of activity) after 35 h on stream indicating a good stability of this catalyst in spite of the carbon content deposited during the reaction (Table 4). NiMo was a little more active than CoMo since, at the same contact time (2.2 min), the initial conversion of 2-EtPh on NiMo was 45 mol%. It seems that the NiMo active phase was less stable than the CoMo active phase during the HDO reaction of 2-EtPh. Indeed after 35 h on stream, a conversion of 38 mol% (16% loss of activity) was observed over NiMo. The deactivation of NiMo could be explained either by coke deposition or by desulfurization of the NiMo active phase. Indeed, Table 4 shows a decrease of the sulfur content on NiMo after reaction. The deactivation of these catalysts during the transformation of 2-EtPh will be presented in an oncoming article.

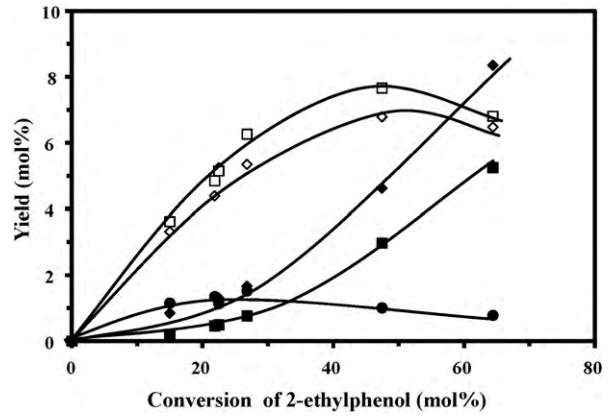

Fig. 5. Transformation of 2-ethylphenol over sulfided Mo/γ-Al_2O_3 catalyst at 340 °C under 7 MPa of total pressure. Effect of the conversion of 2-ethylphenol on the formation of ACI products. Phenol (◊); diethylphenol isomers (□); HDO products from phenol (♦); HDO products from diethylphenol isomers (■); 3-ethylphenol (●).

The products observed over promoted catalysts were the same than those obtained over the unpromoted catalyst, but their yield was very dependent on the promoter used (Fig. 6). For both promoted catalysts, the HYD pathway was the main route for the deoxygenation of 2-EtPh, but it was more significant over NiMo/Al_2O_3 (Fig. 6b) compared to CoMo/Al_2O_3 (Fig. 6a). Moreover, the DDO route was also influenced by the catalyst used. Indeed, for 2-EtPh conversion close to 20 mol%, ethylbenzene represented about 18 mol% of the products for CoMo/Al_2O_3 catalyst and about 4 mol% over NiMo/Al_2O_3 (Table 6).

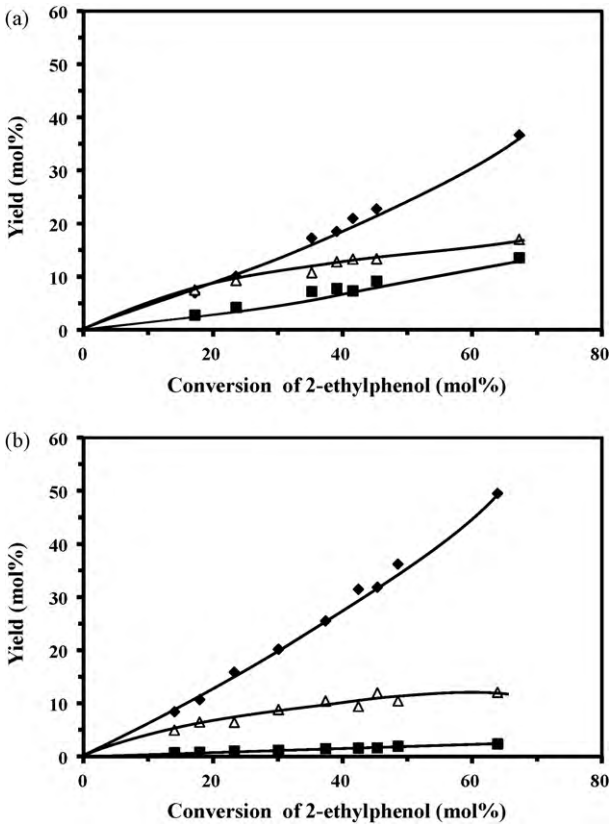

Fig. 6. Transformation of 2-ethylphenol over sulfided CoMo/γ-Al_2O_3 (a) and NiMo/γ-Al_2O_3 (b) at 340 °C under 7 MPa of total pressure. Effect of the conversion of 2-ethylphenol on the product distribution. ACI pathway (△); HYD pathway (♦); DDO pathway (■).

As expected, the presence of nickel or cobalt allowed an increase of the total activity of these catalysts. Both promoted catalysts showed almost the same total activity and were about 1.7 times more active than the unpromoted Mo catalyst (Table 5). The promoting effect in deoxygenation of cobalt and nickel was 2.3 and 2.8, respectively. The promoting effect of nickel was essentially due to the enhancement of the rate of the HYD pathway which was promoted by a factor of 3.4. The presence of cobalt allowed an increase of the products obtained by the two deoxygenation pathways of 2-EtPh, but its effect on the HYD pathway was less significant than for nickel. Indeed, the promoting effect of cobalt on the HYD pathway was about 2 and it was equal to 3.8 on the DDO pathway. In addition, it appears that promoters do not influence the rate of the ACI pathway, as indicated in Table 5.

For a conversion close to 20 mol%, 2-ethylcyclohexane obtained by the HYD pathway was the major product on all catalysts (Table 6). The 1-EtCyHe/3-EtCyHe ratio was similar for the three catalysts used, around 2.8. The presence of promoter changed the contributions of the DDO and the HYD pathways with respect to each other. Indeed, the DDO/HYD selectivity was very dependent on the catalyst used. This selectivity was higher on the catalyst promoted by cobalt, being close to 0.4, and was lower on the catalyst promoted by nickel, close to 0.1.

Over Mo/Al_2O_3 the oxygenated products represented about 85 mol% of all products formed by the ACI pathway and less than 70 mol% for the promoted catalysts. This shows a positive effect of the promoter on the deoxygenation rate of the products formed by isomerization and disproportionation of 2-EtPh. In all cases the main oxygenated product was phenol and the main diethylphenol isomer was 2,6-diethylphenol whichever the catalyst used. Benzene, 1,3-diethylbenzene and 1,4-diethylbenzene were formed in larger amounts over the CoMo than over the NiMo catalyst, indicating that the DDO pathways of phenol and diethylphenols were favored when cobalt was used as promoter, as observed for 2-EtPh.

4. Discussion

4.1. Reaction scheme

The transformation of 2-EtPh over sulfided catalysts promoted by cobalt or nickel and unpromoted catalyst (Mo/Al_2O_3) involved three pathways (Scheme 1). The hydrogenation pathway (HYD) first requires the hydrogenation of the aromatic ring leading to 2-ethylcyclohexanol. This alcohol was not observed in our experimental conditions owing to a rapid dehydration reaction which mainly occurred on the alumina support. However, the contribution of the acidity of the sulfided phase cannot be ruled out. The dehydration of this alcohol led to a mixture of two alkenes (1-ethylcyclohexene and 3-ethylcyclohexene). For all sulfided catalysts used, the amount of 1-ethylcyclohexene was 3 times higher than that of 3-ethylcyclohexene. This ratio was probably imposed by thermodynamics. Indeed the same ratio was also obtained using a NiMoP/Al_2O_3 catalyst for the deoxygenation of 2-EtPh [32] and from the hydrodenitrogenation of indole over NiMo and CoMo catalysts [39]. Moreover, as this ratio was nearly constant over alumina and over sulfided catalysts, this indicates that the rate of hydrogenation of the two alkenes into ethylcyclohexane was about the same. The hydrogenation of such alkenes was very fast in our reaction conditions since ethylcyclohexane was the main product when the conversion of 2-EtPh was above 20 mol%.

The direct deoxygenation pathway (DDO) leads to ethylbenzene through an apparently direct C–O bond scission. In our experimental conditions, the hydrogenation of ethylbenzene into ethylcyclohexane did not occur, indicating that the HYD and DDO pathways are parallel routes. Likewise, at 340 °C under 7 MPa of

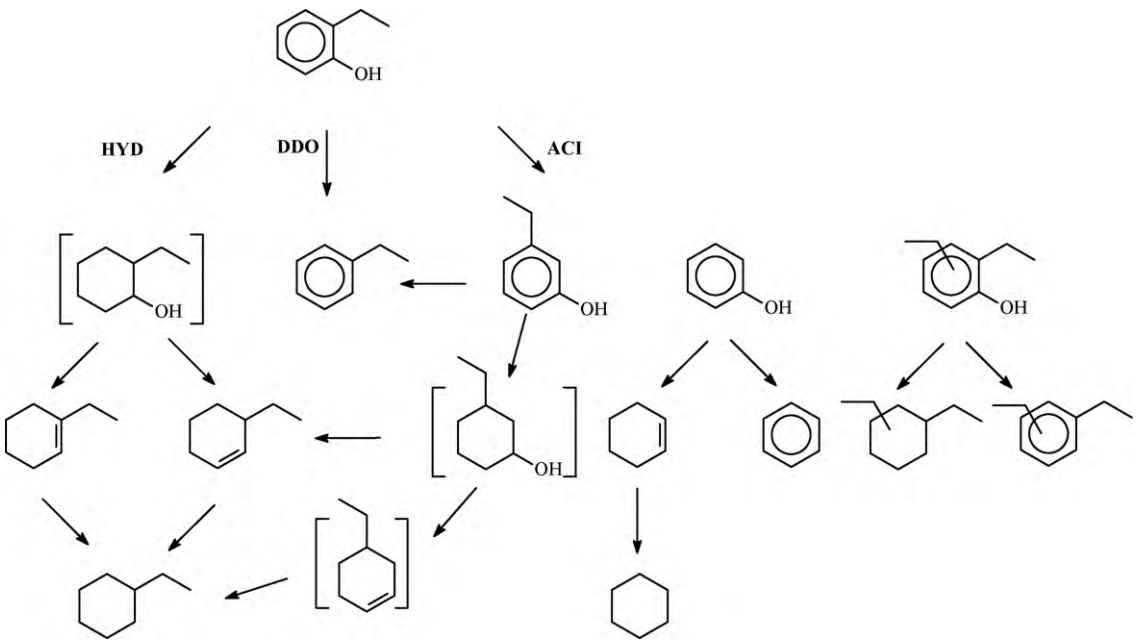

Scheme 1. Transformation of 2-ethylphenol over sulfided Mo-based catalysts. The compounds indicated in brackets were not observed in the reaction mixture.

total pressure, it has been reported that benzene was about 20 times less reactive than phenol in hydrogenation [40].

In addition to these two deoxygenation pathways, a third one was observed which mainly involves the acid properties of the support used (γ-Al_2O_3). Over γ-Al_2O_3 alone, 2-EtPh reacts through disproportionation and isomerization reactions which are typically acid-catalyzed reactions. It has been reported that these kinds of reactions could be catalyzed by alumina [41]. In addition, the presence of H_2S from the decomposition of DMDS could increase the acidity of alumina as already reported [42,43]. The disproportionation of aniline was also observed over sulfided catalysts and was promoted by H_2S [44,45]. The oxygenated compounds formed by these reactions (phenol, 3-EtPh and diethylphenols) were deoxygenated over the sulfided phase.

4.2. Deoxygenation mechanisms and active sites over unpromoted sulfided catalyst

It is generally accepted that the active sites in sulfided catalysts are sulfur vacancies (coordinatively unsaturated sites: CUS) present on the edges of the MoS_2 phase [14]. By DFT calculation, it was shown that the creation of one sulfur vacancy by departure of H_2S is more favorable on the metallic edge than on the sulfur edge over the unpromoted catalyst [46,47]. In addition, taking into account ab initio calculations [48–51], it has been proposed that the shape of MoS_2 slabs is a bulk-truncated hexagon exposing more metallic edges than sulfur edges. As a first approach, the active sites of the unpromoted catalyst for 2-EtPh deoxygenation could be vacancies most likely located on the metallic edge of the MoS_2 slabs. These active sites would be similar for both HYD and DDO pathways. The main difference between these two routes is probably the adsorption mode of the oxygenated molecule on the active site: a DDO center would adsorb 2-EtPh through its oxygen atom whereas a HYD center would adsorb 2-EtPh flat through the aromatic ring.

Scheme 2 presents the proposed mechanism for the DDO pathway. After heterolytic dissociation of H_2 leading to the formation of one S–H and one Mo–H groups, such as already proposed [46,52–54], 2-EtPh could be adsorbed through its oxygen atom on the vacancy discussed above. In the same way, using DFT calculations, it has recently been reported that the η_1 adsorption of furan by the oxygen atom on the metallic edge is more favorable than on the sulfur edge [55]. The addition of a proton to the adsorbed oxygenated molecule leads to an adsorbed carbocation. This intermediate can directly undergo a C–O bond cleavage and the aromatic ring is regenerated leading to ethylbenzene. The vacancy is afterwards recovered by elimination of water.

The mechanism proposed for the HYD pathway is shown in Scheme 3. 2-EtPh can be adsorbed through a η_5 mode through the aromatic ring. As this type of adsorption probably requires more space than η_1 adsorption, the involvement of at least two neighboring vacancies as active site could be proposed for this pathway. For the reasons discussed above, the metallic edge is probably more active than the sulfur edge for the HYD route. After total hydrogenation of the aromatic ring, 2-ethylcyclohexanol is obtained. The dehydration of this alcohol mainly occurs over the acid sites of the alumina, and leads to two cycloalkenes which are hydrogenated into ethylcyclohexane. For simplicity, only the formation and hydrogenation of 1-ethylcyclohexene into ethylcyclohexane are presented in Scheme 3.

Over the unpromoted catalyst, the DDO/HYD selectivity was about 0.2, indicating that the HYD pathway was predominant. If the HYD route requires at least two neighboring vacancies and the DDO pathway only one, 2-EtPh should be more reactive on the DDO route than on the HYD route. As the opposite was observed, the vacancies present on the edges of the MoS_2 slab are probably not the only active sites for the HYD pathway since the presence of neighboring vacancies seems unlikely in presence of H_2S. In fact, it has been proposed that the fully sulfided metallic edges (so-called brim sites) located on the basal plane of the MoS_2 slabs, which contain no vacancies, could be active as hydrogenation sites involved in the desulfurization of thiophene [48,49]. Recently, it was calculated that a flat adsorption of aromatic compounds on the MoS_2 basal plane is possible due to van der Waals interactions [56]. In addition, other sites may also be located at the corners of the slabs. Indeed, by DFT calculation the adsorption of benzene was found more favorable over a corner site of unpromoted tungsten sulfide than over sites present on conventional edges [57].

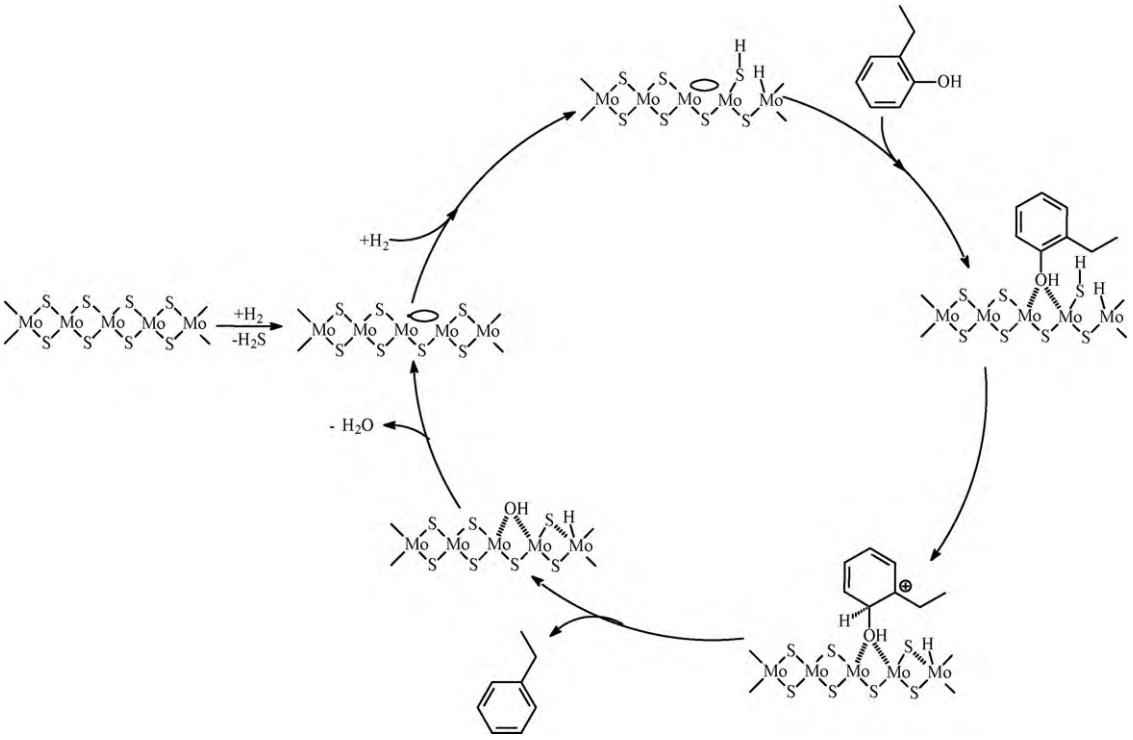

Scheme 2. Mechanism of the direct deoxygenation (DDO) pathway of 2-ethylphenol on a schematic MoS_2-based catalyst.

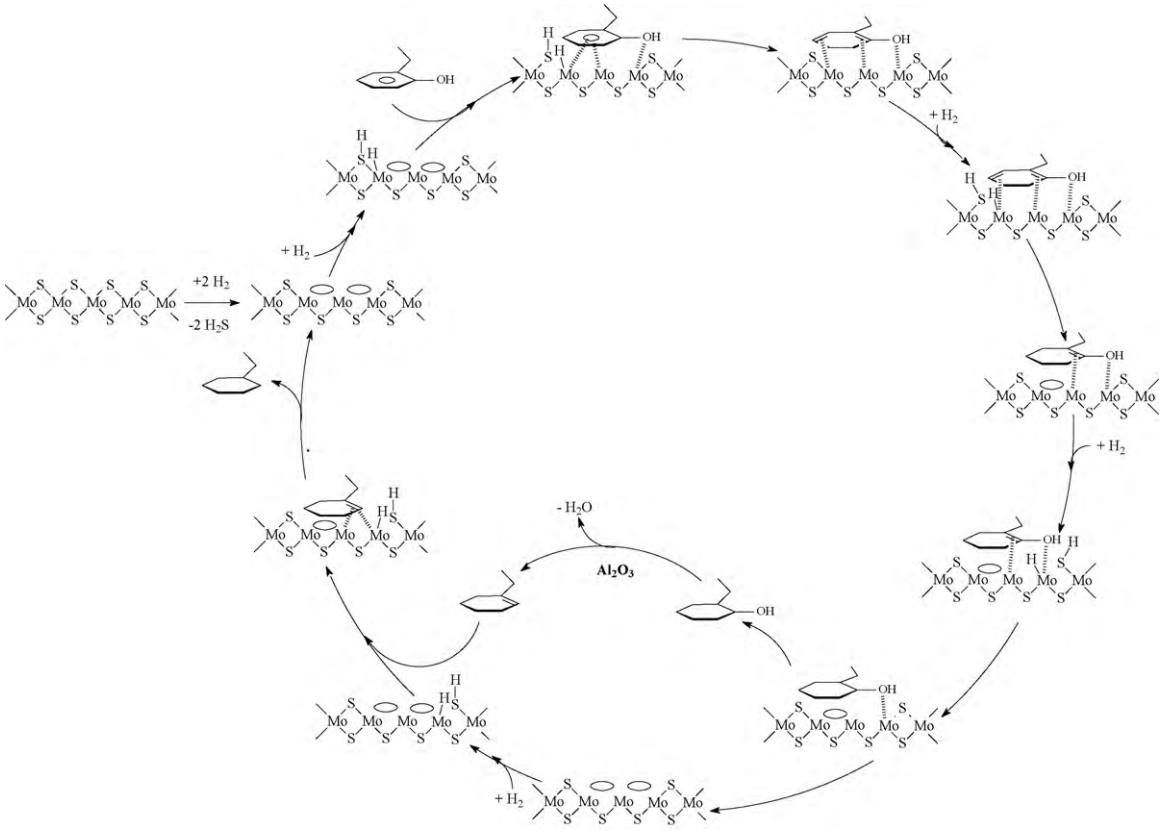

Scheme 3. Mechanism of the hydrogenation (HYD) pathway of 2-ethylphenol on a schematic MoS_2-based catalyst.

4.3. Promoting effect of nickel and cobalt

It is well known that the addition of cobalt and nickel atoms to the sulfided MoS_2 catalyst greatly increases its activity for hydrotreating reactions such as hydrodesulfurization (HDS) and hydrodenitrogenation (HDN) [14]. The results obtained in our study also clearly show a promoting effect of cobalt and nickel for the deoxygenation of 2-EtPh. These promoting effects are represented

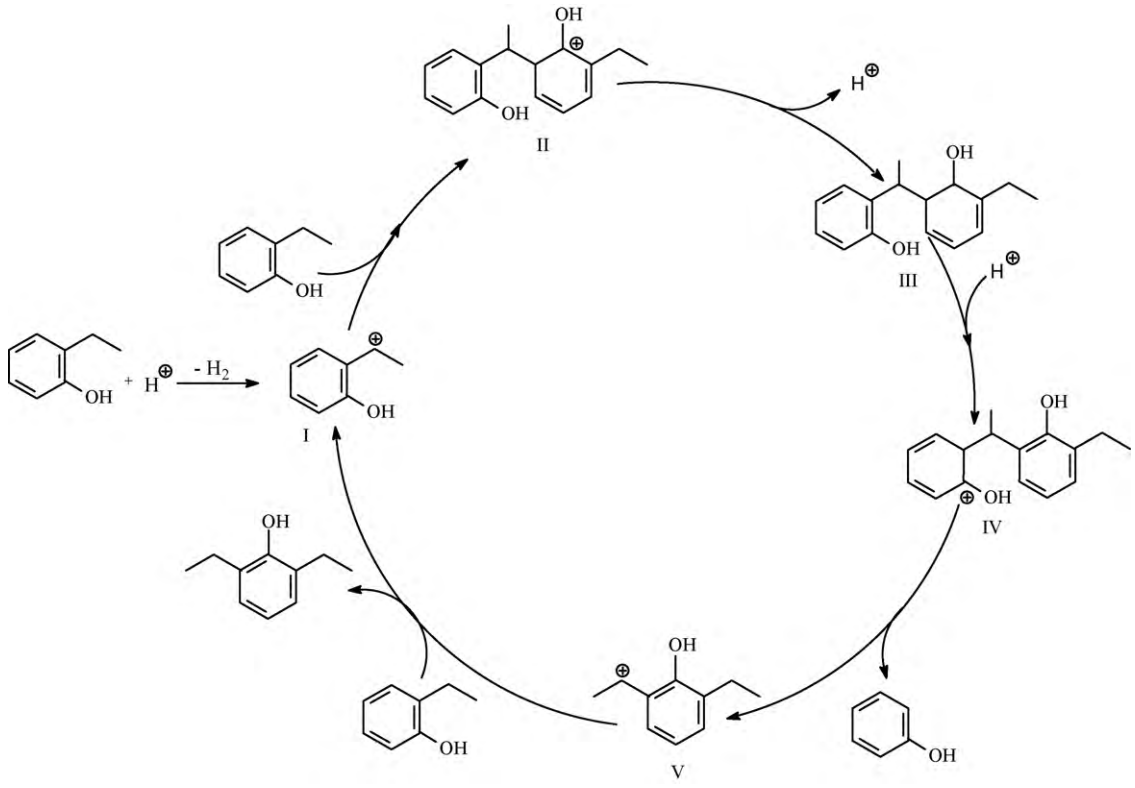

Scheme 4. Mechanism of formation of 2,6-diethylphenol and phenol by disproportionation over γ-Al_2O_3.

by the ratio between the activity of the promoted catalyst and the activity of the unpromoted catalyst (Table 5).

It is now well accepted that the promoting effect of nickel or cobalt is due to an increase in the number of vacancies. Indeed, the promoter (Ni or Co) can donate electrons to molybdenum and lead to a weakening of the metal–sulfur bond [18,19]. The weakening of such a bond has been correlated with the amount of labile sulfur in the active phase (using a ^{35}S radioisotope tracer method) and the addition of promoter enhanced the mobility of sulfur [58–60]. As a consequence, the sulfur atom can be eliminated easily in a promoted catalyst, leading to the creation of more vacancies. Using DFT calculations, it has been confirmed that the most stable position for promoter (Ni or Co) is in substitution of Mo on the edges of the catalyst [51,61–65]. It was proposed that cobalt develops a preferential affinity for the sulfur edge while nickel exhibits a greater affinity for the metallic edge even if it could be localized on both edges, depending on the sulfo-reductive conditions (temperature and molecular ratio H_2S/H_2) [50,51,62,63,65]. In addition, the morphology of CoMoS crystallites is close to a hexagon whereas the morphology of NiMoS crystallites is a deformed hexagon since the NiMoS phase presents a greater amount of metallic edges than sulfur edges.

The promoting effect on the HYD pathway of the 2-EtPh deoxygenation, which mainly implies hydrogenation reactions, was much significant when nickel was used as promoter. $NiMo/Al_2O_3$ catalyst was also found more active than $CoMo/Al_2O_3$ catalyst for the HYD pathway of phenol [29] and 4-methylphenol [24]. Indeed, it is well known that NiMo catalysts are more active for hydrogenation reactions than CoMo catalysts, as already observed for other hydrotreating reactions such as HDS [66,67] and HDN [39] and for hydrogenation of olefins [68–70]. It has been reported that hydrodesulfurization of dibenzothiophene (DBT) and 4,6-dimethyldibenzothiophene occurs via two parallel pathways: the direct desulfurization pathway (DDS) by cleavage of the C–S bond yielding biphenyls and the hydrogenation pathway (HYD) leading to cyclohexylbenzenes [66,67,71–73], which can be compared to the 2-EtPh deoxygenation routes (DDO and HYD, respectively). The promoting effects of nickel and cobalt obtained in our study for the HYD pathway of 2-EtPh are in the same order of magnitude than those obtained for the HYD route of the dibenzothiophenic compounds [66]. The flat adsorption of 2-EtPh required for the HYD route could be easier on bare metal sites which probably exist on the metallic edges promoted by nickel and cobalt. Indeed, it was calculated that the substitution of all the molybdenum atoms by nickel on the metallic edge leads to a stable surface where the nickel atoms are 4-fold coordinated in a square planar environment [64,74]. The HYD route of 2-EtPh is more promoted with the NiMo catalyst probably because the NiMoS phase presents a greater amount of metallic edges than the CoMoS phase, as discussed above. Even though, the participation of brim sites which can be presented in promoted catalysts as proposed by Moses et al. [75] cannot be ruled out.

The promoting effect on the DDO pathway was significant when cobalt was used as promoter, but it was practically not observed in presence of nickel. Consequently the DDO/HYD selectivity was higher on the CoMo catalyst but remained lower than 1, close to 0.4 on the NiMo catalyst. For the HDO of phenolic compounds, several authors [22,24,27] have reported a much higher DDO rate relative to the HYD rate but without H_2S in the feed. For example, Gevert et al. [22] obtained a DDO/HYD selectivity around 4.6 in absence of H_2S in the feed but this selectivity decreased to 0.3 when H_2S was introduced in the reaction mixture. The latter value of selectivity is close to the one reported in the present study, when H_2S was added to the feed in equimolar amount compared to 2-EtPh. The same trend was reported by other authors [24,27], indicating a more important inhibitor effect of H_2S on the DDO pathway than on the HYD pathway.

On the other hand, for dibenzothiophenic compounds, the promoting effect of nickel or cobalt was essentially due to the enhancement of the rate of the DDS pathway [66], which is not observed for the DDO route of 2-EtPh over the NiMo catalyst. This

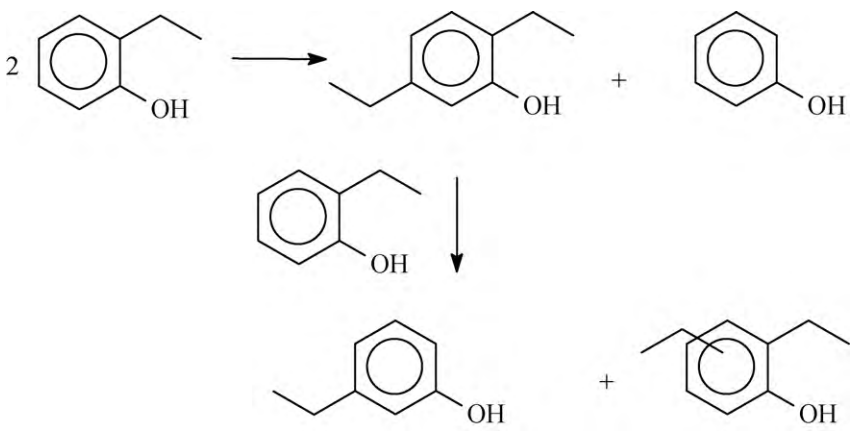

Scheme 5. Isomerization of 2-ethylphenol into 3-ethylphenol through transalkylation.

result is surprising because if the sites involved in the DDO pathway are similar to those involved in the DDS pathway, the former should also be widely promoted by nickel. The difference between the promoting effects of nickel and cobalt on the DDO pathway compared to the DDS pathway could be explained in part by the difference in C–O and C–S bond strength. It has been reported that the C–O bond strength is about 30% higher compared to the C–S bond strength [76]. If the flat adsorption occurs preferentially on promoted metallic edges, the η_1 adsorption mode through the oxygen atom could occur on the sulfur edge. As described above, cobalt prefers to be located at the sulfur edge, this resulting in the creation of more vacancies on this edge, which could be active in the production of ethylbenzene (DDO route). This is in accordance with the proposal made by several authors [64,77] who suggested that the sulfur edge is the more active for the direct bond scission of C–S.

4.4. Disproportionation and isomerization mechanisms

The disproportionation mechanism of 2-EtPh is depicted in Scheme 4. This mechanism is in accordance with that reported for the disproportionation of sulfur compounds [78,79] as well as with the proposals made for toluene and m-xylene disproportionation [80,81]. For the sake of simplicity, this scheme is limited to the formation of 2,6-diethylphenol and phenol. In the initial step, adsorbed 2-EtPh reacts with a proton and loses a methyl hydrogen to form H_2 and a carbocation of benzyl-type (4-I), which reacts with another 2-EtPh molecule to form a bimolecular intermediate (4-II). After deprotonation the dimer 4-III is formed, and leads by re-adsorption and protonation of the second phenolic ring to the 4-IV intermediate. After bond scission, phenol and the ion 4-V are formed. This ion can substract a hydride from another 2-EtPh and desorb, leading to 2,6-diethylphenol. The differences in the distribution of the diethylphenol isomers observed in Fig. 3 could be explained by the stability of the carbenium ions of type 4-II, as reported for the disproportionation of thiophenic compounds [79].

Isomerization reactions can occur via an intramolecular or an intermolecular mechanism. Intramolecular isomerization involves a 1,2 ethyl shift while intermolecular isomerization occurs via transalkylation reactions. As isomerization products were secondary, the contribution of the intramolecular mechanism was always of minor importance compared to the intermolecular mechanism (Scheme 5). Indeed it was reported that the intermolecular mechanism becomes predominant when the catalyst has only weak acid sites [80].

5. Conclusions

The activity for hydrodeoxygenation of 2-ethylphenol, a model molecule representative of oxygenated compounds present in biocrude, was measured on sulfided (Ni or Co)Mo/Al_2O_3 catalysts under conditions close to those of conventional hydrotreatment process (7 MPa and 340 °C). Over sulfided catalysts, the overall promoting effect of nickel was slightly higher than that of cobalt. The deoxygenation of 2-ethylphenol took place by two parallel routes: the HYD pathway yielding mainly ethylcyclohexane and the DDO pathway yielding only ethylbenzene. For all the studied catalysts, the HYD pathway was the main route of the deoxygenation of 2-EtPh. Compared to sulfided Mo/Al_2O_3, promotion by nickel markedly favors hydrogenation activity of the catalyst (promoting factor of 3.4), whereas cobalt promotion mainly enhances the direct C–O bond scission activity (promoting factor of 3.8). Therefore, the highest DDO/HYD selectivity was obtained for CoMo/Al_2O_3. The promoting effects observed were explained by an increase of the number of active sites, some of them being new sulfur vacancies.

The HYD pathway implies first a flat adsorption by the aromatic ring whereas the DDO pathway first requires an adsorption through the oxygen atom. Both adsorptions could occur on sulfur vacancies, which are located on metallic and sulfur edges of promoted catalysts, and likely only on metallic edges of an unpromoted catalyst. As sulfur vacancies are probably sparse over the latter, fully sulfided metallic edges (so-called brim sites) presents on the basal plane of the MoS_2 slabs could also participate as active sites in the HYD pathway of the unpromoted catalyst. Over promoted catalysts, metallic edges could be active in the HYD pathway whereas sulfur edges are more likely responsible for the DDO pathway.

The acidity of the alumina plays a role in the transformation of 2-ethylphenol leading to disproportionation and isomerization products. The disproportionation reaction is supposed to occur through a bimolecular cationic mechanism. The isomerization reaction occurs by an intermolecular mechanism involving transalkylation reactions. Over the sulfided phases, these products are also deoxygenated via both HYD and DDO pathways.

This preliminary study on the 2-EtPh transformation over Mo/Al_2O_3-sulfided based catalysts has allowed measuring the promoting effect of cobalt and nickel for the HDO of a phenolic compound over supported catalysts. To a better understanding of the role of the promoter, as well as the evaluation of the intrinsic activity of the active phase, more characterization studies such as CO adsorption followed by IR are being considered.

Acknowledgements

This work has been performed within the ANR funded Programme National de Recherche sur les bioénergies-ECOHDOC, a joint project of the Centre National de la Recherche Scientifique (CNRS), the Universities of Caen, Lille and Poitiers, and Total.

References

[1] C. Di Blasi, Prog. Energy Combust. Sci. 34 (2008) 47.
[2] D.O. Hall, For. Ecol. Manage. 91 (1997) 17.
[3] Official J. Eur. Union L140 (2009) 88.
[4] L. Wei, S. Xu, L. Zhang, H. Zhang, C. Liu, H. Zhu, S. Liu, Fuel Process. Technol. 87 (2006) 863.
[5] D. Mohan, C.U. Pittman, P.H. Steele, Energy Fuels 20 (2006) 848.
[6] A.G.W. Huber, S. Iborra, A. Corma, Chem. Rev. 106 (2006) 4044.
[7] A. Demirbas, Prog. Energy Combust. Sci. 33 (2007) 1.
[8] D.C. Elliot, Energy Fuels 21 (3) (2007) 1792.
[9] O. Senneca, Fuel Process. Technol. 88 (2007) 87.
[10] L. Ingram, D. Mohan, M. Bricka, P. Steele, D. Strobel, D. Crocker, B. Mitchell, J. Mohammad, K. Cantrell, C.U. Pittman, Energy Fuels 22 (2008) 614.
[11] J.H. Marsman, J. Wildschut, F. Mahfud, H.J. Heeres, J. Chromatogr. A 1150 (2007) 21.
[12] J.H. Marsman, J. Wildschut, P. Evers, S. de Koning, H.J. Heeres, J. Chromatogr. A 1188 (2008) 17.
[13] E. Furimsky, Appl. Catal. A: Gen. 199 (2000) 147.
[14] H. Topsøe, B.S. Clausen, F.E. Massoth, Hydrotreating Catalysis, Science and Technology, vol. 11, Springer Verlag, 1996.
[15] H. Topsøe, B.S. Clausen, R. Candia, C. Wivel, S. Morup, J. Catal. 68 (1981) 433.
[16] C. Wivel, R. Candia, B.S. Clausen, S. Morup, H. Topsøe, J. Catal. 68 (1981) 453.
[17] H. Topsøe, B.S. Clausen, Catal. Rev.: Sci. Eng. 26 (1984) 395.
[18] R.R. Chianelli, Catal. Rev.: Sci. Eng. 26 (1984) 361.
[19] S. Harris, R.R. Chianelli, J. Catal. 98 (1986) 17.
[20] E. Odebunmi, D. Ollis, J. Catal. 80 (1983) 56.
[21] E. Furimsky, J. Mikhlin, D. Jones, T. Adley, H. Baikowitz, Can. J. Chem. Eng. 64 (1986) 982.
[22] B.S. Gevert, J. Otterstedt, F.E. Massoth, Appl. Catal. 31 (1987) 119.
[23] C. Aubert, R. Durand, P. Geneste, C. Moreau, J. Catal. 112 (1988) 12.
[24] E. Laurent, B. Delmon, Ind. Eng. Chem. Res. 32 (1993) 2516.
[25] B.S. Gevert, M. Eriksson, P. Eriksson, F.E. Massoth, Appl. Catal. A: Gen. 117 (1994) 151.
[26] E. Shin, M. Keane, J. Catal. 173 (1998) 450.
[27] T.-R. Viljava, R.S. Komulainem, A.O.I. Krause, Catal. Today 60 (2000) 83.
[28] F.E. Massoth, P. Politzer, M.C. Concha, J.S. Murray, J. Jakowski, J. Simons, J. Phys. Chem. B 110 (2006) 14283.
[29] O.I. Senol, E.-M. Ryymin, T.-R. Viljava, A.O.I. Krause, J. Mol. Catal. A: Chem. 277 (2007) 107.
[30] Y.Q. Yang, C.T. Tye, K.J. Smith, Catal. Commun. 9 (2008) 1364.
[31] I. Gandarias, V.L. Barrio, J. Requies, P.L. Arias, J.F. Cambra, M.B. Güemez, Int. J. Hydrogen Energy 33 (2008) 3485.
[32] Y. Romero, F. Richard, Y. Renème, S. Brunet, Appl. Catal. A: Gen. 353 (2009) 46.
[33] C.N. Satterfield, S.H. Yang, J. Catal. 81 (1983) 335.
[34] C. Lee, D. Ollis, J. Catal. 87 (1984) 325.
[35] M.C. Edelman, M.K. Maholland, R.M. Baldwin, S.W. Cowley, J. Catal. 111 (1988) 243.
[36] A.Y. Bunch, U.S. Ozkan, J. Catal. 206 (2002) 177.
[37] A.Y. Bunch, X. Wang, U.S. Ozkan, J. Mol. Catal. A: Chem. 270 (2007) 264.
[38] A.Y. Bunch, X. Wang, U.S. Ozkan, Appl. Catal. A: Gen. 346 (2008) 96.
[39] S.C. Kim, F.E. Massoth, J. Catal. 189 (2000) 70.
[40] C. Moreau, C. Aubert, R. Durand, N. Zmimita, P. Geneste, Catal. Today 4 (1988) 117.
[41] M. Jayamani, C.N. Pillai, J. Catal. 82 (1983) 485.
[42] C. Arrouvel, H. Toulhoat, M. Breysse, P. Raybaud, J. Catal. 226 (2004) 260.
[43] A. Travert, O.V. Manoilova, A.A. Tsyganenko, F. Maugé, J.C. Lavalley, J. Phys. Chem. B 106 (2002) 1350.
[44] J. van Gestel, J. Leglise, J.-C. Duchet, Appl. Catal. A: Gen. 92 (1992) 143.
[45] J. van Gestel, C. Dujardin, F. Maugé, J.C. Duchet, J. Catal. 202 (2001) 78.
[46] J.-F. Paul, E. Payen, J. Phys. Chem. B 107 (2003) 4057.
[47] M. Sun, A.E. Nelson, J. Adjaye, Catal. Today 105 (2005) 36.
[48] J.V. Lauritsen, M.V. Bollinger, E. Laegsgaard, K.W. Jacobsen, J.K. Nørskov, B.S. Clausen, H. Topsøe, F. Besenbacher, J. Catal. 221 (2004) 510.
[49] J.V. Lauritsen, J. Kibsgaard, G.H. Olesen, P.G. Moses, B. Hinnemann, S. Helveg, J.K. Nørskov, B.S. Clausen, H. Topsøe, E. Laegsgaard, F. Besenbacher, J. Catal. 249 (2007) 220.
[50] H. Schweiger, P. Raybaud, H. Toulhoat, J. Catal. 212 (2002) 33.
[51] P. Raybaud, Appl. Catal. A: Gen. 322 (2007) 76.
[52] S. Kasztelan, D. Guillaume, Ind. Eng. Chem. Res. 33 (1994) 203.
[53] C. Thomas, L. Vivier, J.L. Lemberton, S. Kasztelan, G. Pérot, J. Catal. 167 (1997) 1.
[54] S. Blanchin, P. Galtier, S. Kasztelan, S. Kressmann, H. Penet, G. Pérot, J. Phys. Chem. A 105 (2001) 10860.
[55] M. Badawi, S. Cristol, J.-F. Paul, E. Payen, C. R. Chim. 12 (2009) 754.
[56] P.G. Moses, J.J. Mortensen, B.I. Lundqvist, J.K. Norskov, J. Chem. Phys. 130 (2009) 104709.
[57] R. Koide, E.J.M. Hensen, J.-F. Paul, S. Cristol, E. Payen, H. Nakamura, R.A. van Santen, Catal. Today 130 (2008) 178.
[58] W. Qian, Y. Hachiya, D. Wang, K. Hirabayashi, A. Ishihara, T. Kabea, H. Okazaki, M. Adachi, Appl. Catal. A: Gen. 227 (2002) 19.
[59] V. Kogan, A. Greish, G. Isagulyants, Catal. Lett. 6 (1990) 157.
[60] V. Kogan, N. Rozhdestvenskaya, I. Korshevets, Appl. Catal. A: Gen. 234 (2002) 207.
[61] P. Raybaud, J. Hafner, G. Kresse, S. Kasztelan, H. Toulhoat, J. Catal. 190 (2000) 128.
[62] F. Besenbacher, M. Brorson, B.S. Clausen, S. Helveg, B. Hinnemann, J. Kibsgaard, J.V. Lauritsen, P.G. Moses, J.K. Nørskov, J.-H. Topsøe, Catal. Today 130 (2008) 86.
[63] E. Krebs, B. Silvi, P. Raybaud, Catal. Today 130 (2008) 160.
[64] J.-F. Paul, S. Cristol, E. Payen, Catal. Today 130 (2008) 139.
[65] M. Sun, A.E. Nelson, J. Adjaye, J. Catal. 226 (2004) 32.
[66] F. Bataille, J.L. Lemberton, P. Michaud, G. Pérot, M. Vrinat, M. Lemaire, E. Schulz, M. Breysse, S. Kasztelan, J. Catal. 161 (2000) 409.
[67] M. Egorova, R. Prins, J. Catal. 225 (2004) 417.
[68] A.-F. Lamic, A. Daudin, S. Brunet, C. Legens, C. Bouchy, E. Devers, Appl. Catal. A: Gen. 344 (2008) 198.
[69] M. Brémaud, L. Vivier, G. Pérot, V. Harlé, C. Bouchy, Appl. Catal. A: Gen. 289 (2005) 44.
[70] M. Badawi, L. Vivier, G. Pérot, D. Duprez, J. Mol. Catal. A: Chem. 293 (2008) 53.
[71] M. Houalla, N.K. Nag, A.V. Sapre, D.H. Broderick, B.C. Gates, AIChE J. 24 (1978) 1015.
[72] G.H. Singhal, R.L. Espino, J.E. Sobel, G.A. Huff, J. Catal. 67 (1981) 457.
[73] F. Richard, T. Boita, G. Pérot, Appl. Catal. A: Gen. 320 (2007) 69.
[74] A. Travert, C. Dujardin, F. Maugé, E. Veilly, S. Cristol, J.-F. Paul, E. Payen, J. Phys. Chem. B 110 (2006) 1261.
[75] P.G. Moses, B. Hinnemann, H. Topsøe, J.K. Nørskov, J. Catal. 268 (2009) 201.
[76] J. March, Advanced Organic Chemistry, third ed., John Wiley & Sons, New York, 1985, p. 23.
[77] P.G. Moses, B. Hinnemann, H. Topsøe, J.K. Nørskov, J. Catal. 248 (2007) 188.
[78] T. Boita, M. Moreau, F. Richard, G. Pérot, Appl. Catal. A: Gen. 305 (2006) 90.
[79] F. Richard, T. Boita, M. Moreau, C. Bachmann, G. Pérot, J. Mol. Catal. A: Chem. 237 (2007) 48.
[80] M. Guisnet, N.S. Gnep, S. Morin, Microporous Mesoporous Mater. 35–36 (2000) 47.
[81] L.A. Clark, M. Sierka, J. Sauer, J. Am. Chem. Soc. 125 (2003) 2136.